An analysis of metal wear in rock excavation by TBM

(Article begins on next page)

15 May 2024

An analysis of metal wear in rock excavation by TBM

M. Cardu, A. Di Giovanni & S. Saltarin
DIATI Politecnico di Torino, Italy

C. Todaro
IGG-CNR, Torino, Italy

ABSTRACT: Abrasivity, or its reciprocal concept, "wear resistance", are not intrinsic properties of a material, but rather parameters describing the interaction of two materials, i.e. the wear part and the material exerting the wearing action. Moreover, "wear" or, at least, that part of the wear, which is due to the cumulated effect of minute scratches, is linked to the "hardness disparity" concept: an example is provided by the well-known Mohs hardness scale (the "harder" body wears the "softer" body). In the case of rock-metal interaction, a difficulty arises from the inhomogeneity of the interacting bodies. The paper, after a synthetic explanation of the basic principles, deals first with the problem of measuring and representing the hardness of inhomogeneous bodies; a simple procedure is described, with practical examples. Then, after a review of data on TBM disc service life and rock abrasivity evaluation, cases of TBM used in hydropower tunnel driving in Italy are presented. Data pertaining to the rock bored and to the metal composing the discs, together with machine data, tools consumption and machine productivity are provided and compared to find correlations enabling to forecast tools service life.

1   INTRODUCTION

Excavation and/or drilling tools' service life is mainly affected by the amount of work the tool is required to provide in unit time. Large amounts of metals are consumed in rock excavation. Metal wastage can be ascribed to: 1. worn metal due to the excavation; 2. residual mass of discarded worn parts; 3. breakages and broken parts replacement; 4. obsolete machinery and plant replacement. Reference is here made to point 1; it must be warned, however, that in metals an increase in wear resistance is usually accompanied by a decrease in toughness (Bai et al. 2021), while in rocks the opposite is usually true. The wear/breakage interplay is very complicated, being usually breakage partly a consequence of wear. The wear/breakage borderline is arbitrarily set and how large and severe must be the damage to be considered breakage instead of wear is debatable. Lastly, wear is not merely due to mechanical problems since also tribochemical effects (corrosion enhanced by mechanical wear and vice-versa), play an important role. Anyhow, wear can be considered as the result of minute mechanical failures. Strength and hardness characterize the rock or the metal with respect to the resistance to mechanical damage (breakage, wear). However, the pair (metal/rock) should be characterized when dealing with interactions.

Metal loss includes the effects of tool-rock interactions that occur on the microscale ("wear" in the strict sense) and on a larger scale ("breakages" of the tool, due to a too-high force applied to the tool). However, the two "scales" and consequently wear and breakages are strictly connected. Intuitively, a worn tool requires more thrust to function, which makes breakage more likely. To prevent or reduce wear, the hardness of the tool can be increased but, as already stated, a growth in hardening usually leads to an increase in metal brittleness, which has a negative effect on the frequency of breakage (Pal Dey & Deevi 2003). Other possibilities consist in using additives

expressly designed to create a layer between the tool and the surface that has to be excavated for wear reduction (Oñate Salazar et al. 2016a, Di Giovanni et al. 2022) but not always this is realizable for environmental restrictions.

As far as wear is concerned, the most common approach is to characterize the rock's "abrasivity" based on its mineralogical composition (Oñate Salazar et al. 2016b, Todaro et al. 2022), which leads to the "equivalent quartz content" (Schimanek 1970), that is a practical, though not rigorous, rock characterization criterion. The approach here used is intended to represent a second approximation criterion: being tool hardness variable as well as rock hardness, the "rock-metal" pair can be characterized by means of the "hardness ratio", instead of characterising the rock only (Cardu & Giraudi 2012).

Indicators of the stress levels leading to failure are commonly employed to characterise materials at the macroscopic scale, as the uniaxial compression strength or the shear strength. Instead, when considering the problem of characterisation at a very small size scale, two difficulties arise: the so-called size or scale effects (dependence of the measured strength values on the size of the probe) and the small-scale inhomogeneity of the materials (Mancini et al. 1993).

The first difficulty has been overcome through the systematic use of micro-scale mechanical testing that permits to measure the micro-hardness (Frisa Morandini & Mancini 1982). Besides different methodologies characterized by different shapes of the bit used for the micro-hardness assessment, the Knoop test has become the reference, since it can be used to measure the hardness of metals as well as of minerals, rocks, glasses and ceramics, the only constraint being posed by the polishability of the probe. Hardness values quoted in this report are obtained with a Leitz Durimet testing at least one machine equipped with a Knoop penetrator; a load equal to 200 g (1.962 N), in compliance with the Italian regulations (UNI 9724 part 6), was applied to the bit. The size of the domains mechanically characterized by a micro-hardness test is typically in the 10 - 100 micrometers range.

The second difficulty has been solved by adopting a statistical representation (frequency distribution diagram) of the measured punctual hardness values, represented on a semi-logarithmic scale. A reproducible distribution diagram can be drawn based on at least 40 readings, even in inhomogeneous materials (i.e. granitic rocks). Diagrams presented in this report are obtained according to the suggested number of readings, both for rocks and for metals. Examples are shown in Figure 1. To be noticed the significant inhomogeneity at the micro-metric scale, featured by visually homogeneous materials like metals. Only homogeneous glasses are exempt from small-scale inhomogeneity. In the case of TBMs, the well-known and theorized dependence of the disk replacement on its position (center, mid, periphery) on the TBM head can be explained simply by the different amounts of excavation work allocated to the different discs. Apart from that, tool service life depends on the "sensitivity" to the metal loss of the tool, which means, the amount of metal loss tolerated without serious impairment of the efficiency (for example, drag bits are more sensitive than discs, and small discs more sensitive than large discs). Lastly, service life depends, jointly, on the rock excavated and on the metal employed to make the tools (Oñate Salazar et al. 2018).

2 ROCK-METAL PAIR MECHANICAL CHARACTERIZATION

It is assumed that, during operation, the rock elements and the metal parts come in contact repeatedly, and that instantaneous contact points are randomly distributed on the rock elements and on the metal parts. The hardness ratio between metal and rock at the contact point is linked to the severity of the elementary wear event. The pair can be therefore characterized by the cumulated frequency distribution diagram of the –metal-rock hardness ratio at randomly distributed contact points. As already reported, the diagram can be obtained by 40 metal and 40 rock hardness values employed to characterize the individual materials: it consists of a total number of 1600 equiprobable hardness ratio values (R). As an example, Figure 2 depicts two curves related to the micro-hardness cumulated frequency distribution of a serpentinite (1) and of the steel of which the employed jaw crusher is made up (2). Figure 3 instead reports the 1600 equiprobable hardness ratio values (R) and the relative cumulated frequency distribution. The
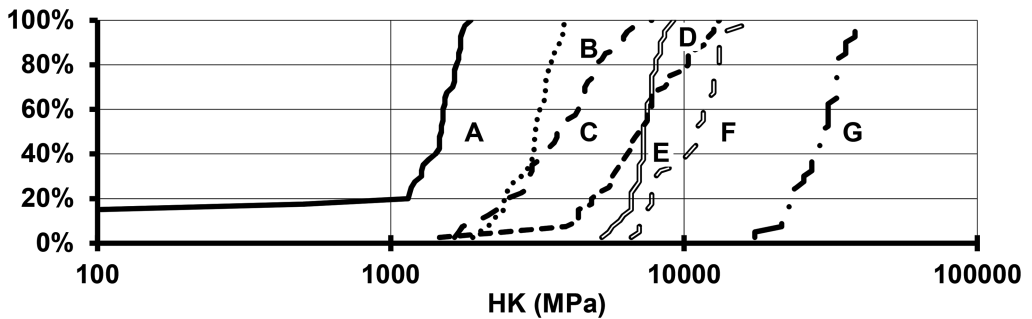
Figure 1. Examples of microhardness frequency distribution diagrams. Semilog charts are employed due to the extremely wide hardness range. A: travertine (negligible hardness points, amounting to 18-20 %, are pores); B: dolomitic limestone; C: serpentinite; D: fine-grained white granite; E: hard steel, from a crusher jaw; F: hard steel, from a TBM disc; G: sintered carbide prism, from stone chain cutter.

diagrams so drawn proved to be highly reproducible. The hardness ratio distribution diagram can show how frequent are random contacts where the hardness ratio between metal and rock falls below a "safe limit" excluding damage to the wear part; the more displaced towards the right is the diagram, the less serious should be the wear problem. When R is lower than 1, the microhardness of the rock is higher than that of one of the steel tools.

   TBM discs pose a special problem, because both wear and breakage are important causes of service life-shortening and, moreover, are interacting causes: wear forces to increase
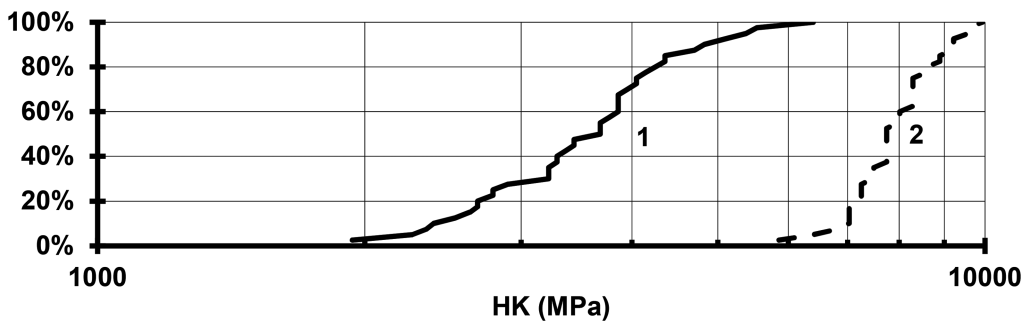

Figure 2. Micro-hardness cumulated frequency distribution diagrams for a serpentinite (A) quarried for railroad ballast, and for the steel tools (B) of which the jaws of the crusher employed are composed.
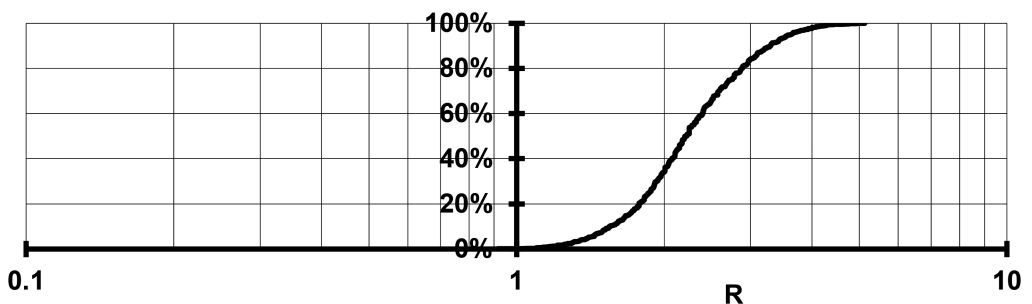

Figure 3. Hardness ratio distribution diagram for case of Figure 2.

thrust (since the disk starts to not work properly), and increased thrust makes breakages more likely.

In the following, 4 different real cases are described. Cases are identified with capital letters A-B and general data related to the tunnels' excavation are reported in Table 1.

Hardness analysis of the cross-section of the discs reveals different metal hardening strategies: in some cases, the same hardness distribution diagram is obtained, irrespective of the distance of the tested area from the cutting edge, in other cases (case A) the metal close to the cutting edge is harder than the core (Figure 4). Analysing Figure 4, it can be deemed that a different hardening process has been employed in order to save the toughness of the core metal.

Figures 5-6 refer to cases B and D (hydropower tunnels). As reported in Table 1, rocks were a dolomitic limestone in case B and a hard gneiss in case D. A somewhat harder, but not dif-
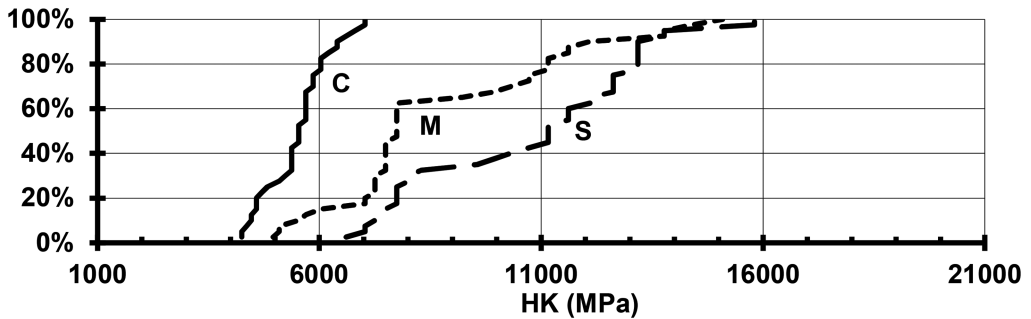

Figure 4. Hardness distribution diagram obtained from tests on different parts of the cross-section of the cutting ring of the TBM disc of case A. S: testing area close to the cutting edge (down to 1 cm depth); C: the core of the ring; M: 40 points randomly distributed in the cross-section.

ferent hardened, steel was selected for the discs employed in the latter case. Tunnel B was successfully driven, with reasonable tool consumption (0.0022 discs/m^3, see Table 3) while case D was unsuccessful. In detail, in case D operation was discontinued at 30 m chainage, being all discs out of service (the rock was probably beyond the practical limit for steel discs).
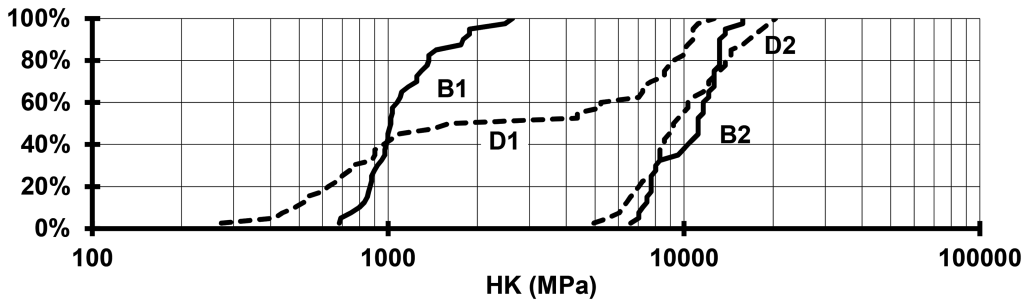

Figure 5. Rock and metal hardness distribution diagrams for the two TBM operations: B1: dolomitic limestone; B2: TBM disc employed in dolomitic limestone boring; D1: hard gneiss; D2: TBM disc employed (failed attempt).
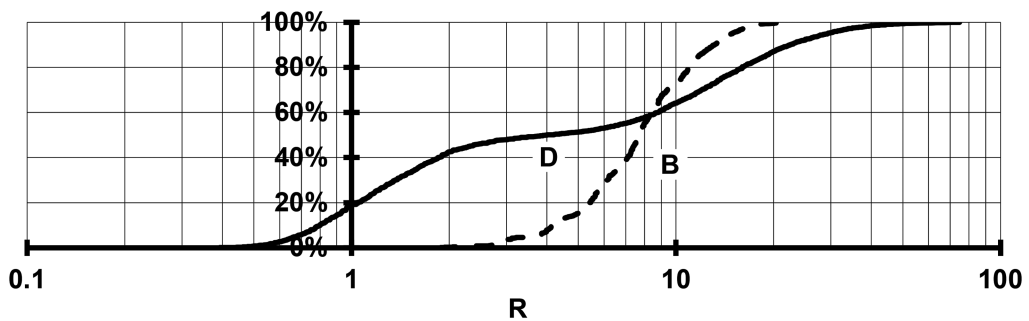
Figure 6. Hardness ratio distribution diagrams for the two cases of Figure 5. B: steel B2 v/ dolomitic limestone B1; D: steel D2 v/ gneiss D1. The problem related to case D can be easily noticed, where the hardness of the metal is lower than that of the rock in ~20% of the interactions. In fact, case D was unsuccessful.

3 TOOL WEAR IN TBM EXCAVATION

TBM practical advance rate depends on the net advance rate and on the idle time, which is accounted for by means of a "machine utilization coefficient". While the net advance rate is mainly dictated by rock strength and is comparatively easy to predict, the utilization coefficient depends on a so large number of factors that reliable predictions are very difficult to make. Metal wear is only one of the factors on which the utilization coefficient depends and can represent a negligible or a very important factor according to the operation considered (Ribacchi & Fazio 2005). Anyhow, an improvement of the rock abrasivity characterization should represent important progress, at least for this part of the general problem. The names of the operations have been omitted: cases are labeled as tunnels A, B, C1, C2, and D (see Table 1).

In the case A, the machine did not complete the tunnel due to the very high abrasiveness of the rock encountered at chainage 1900 m (hard granitic gneiss and anatexites). The tunnel in case B was completed with success in limestone (distinctly bedded, faulted, and folded, with marl and clay partings) and in a massive and hard dolomitic limestone.

As for tunnel C (14800 m long), two stretches are examined (C1, 3651 m and C2, 3790 m long) that were excavated in calcschists, micaschists, and meta-conglomerates without problem, except in intensively faulted and folded rocks with the presence of shear zones. In tunnel D, an incline of around 40° slope, both the machine and the tools were not suitable for the tough and abrasive rocks to cross (amphibolites, pegmatites, and amphibolitic gneiss) and therefore it was necessary to replace the machine, but the data are not available in this regard.

The data of the machine are collected in Table 2, performance data in Table 3, and rock data in Table 4.

Table 1. General data related to the tunnels' excavation.

Tunnel	D	L_1	L_2	Lithotype	Days to complete the tunnel	H
A	2.57	6215	1900	Granitic gneiss	224	/
B	3.5	3052	2981	Dolomitic limestone	134	400
C1-C2	3.5	14800	14800	Calcschist, micaschist Meta-conglomerate	281 + 198	500
D	3.6	752	20	Amphibolitic gneiss	/	150*

* Measured perpendicularly from the sloping surface of the mountain

1187

D = tunnel diameter (m); L1 = tunnel length (m); L2 = length excavated by TBM (m); H = Average overburden thickness (m).

Table 2.   Machines' data.

Machine	D	S	T_{max}	T_{av}	N	ϕ	n	P_{max}	P_{av}	Total Power
A	2.57	0.7	2800	1800-2000	17*	300	12	380	160	380
B	3.5	0.75	7155	4000	27	397	9.57	552	480	680
C1-C2	3.5	1.5	6200	3960	26	412	10.6	600	504	900
D	3.6	1.16	4440	/	33	412	12	390	/	460

* Double disc tools.

D = head diameter (m); S = maximum stroke (m); T_{max} = maximum thrust (kN); T_{av} = average thrust during excavation (kN); N = number of tools (-); ϕ = tool diameter (mm); n = head revolutions per minute (rpm); P_{max} = maximum power at the head (kW); P_{av} = average power at the head during operation (kW); Total Power (kW).

Table 3.   Machines' performance data.

Case	N. P. R.	U. C.	A. D. P.	E_s	S. T. C.
A	1.13	0.31	8.47	27	0.021
B	3.7	0.38*	22.2	13.5	0.0022
C1-C2	2.4	0.27**	20	23	0.0035
D	/	/	/	/	/

* Calculated on the worked days.
** Rock reinforcement time is not considered.

N.P.R. = Net Progression Rate (m/h); U.C. = Utilisation Coefficient (-); A.D.P. = Average Daily Progression (m/d); Es = Specific Power Consumption (kWh/m3); S.T.C. = Specific Tools Consumption (tools/m3).

Table 4.   Geomechanical characteristics of the rocks encountered by the tunnels.

Case	C_0	T_0	RMR	HK_{75}	s/q
A	70-170	7-12	70-85	5990	0.138
B	60-180	5	60-80	1500	0.002
C1-C2	60-130	5-7	30-70	6300	0.083-0.16
D	90-200	10-16	60-80	8200	0.05-0.08

C_0 = Uniaxial strength of the rock (MPa); T_0 = Tensile strength (MPa) (Brazilian test); RMR = Rock Mass Rating (-); HK_{75} = micro-hardness of the tools' steel (MPa); s/q = the result of the drillability test with a small diameter bit (mm-1) (more details are provided in the following).

3.1   *Performance of the machine*

Table 3 shows that the net progression rate was generally pretty good, though being affected by machine features and by rock characteristics. The interrelation between the variables is complicated, being involved several parameters, mainly pertaining to the machine.

The description of the behavior of the TBM can however be synthesized, as far as the net progression rate is concerned, with the relationships linking three dimensionless ratios, that are: p/ϕ, C_0/E_s, $T/(A*E_s)$, where p is TBM's penetration per revolution (mm), ϕ is the disc diameter (mm), E_s is the specific energy (MJ/m^3), T the thrust (MN), A is the cross-section of the tunnel (m^2). In Figures 7-8, p/ϕ is plotted against C_0/E_s and $T/(A*E_s)$ respectively. With reference to Table 1, only cases A, B, and C were considered for the analysis. Despite the wide scatter, both suggest linear relationships that can be synthesized with equations (1) and (2):

$$T/(A*E_s) \sim 0.5 \; p/\phi \tag{1}$$

$$C_0/E_s \sim 100 \; p/\phi \tag{2}$$

from which semi-quantitative relationships and predictions can be easily derived:

1. $T \sim 0.005 \; (A * C_0)$, which roughly agrees with the observed data: actually $T = 0.0053 \pm 0.0019 \; (A * C_0)$.
2. T, A, and ϕ being equal, E_s decreases as p increases.
3. p and ϕ being equal, E_s grows as C_0 grows, and E_s and C_0 being equal, p grows as ϕ grows.

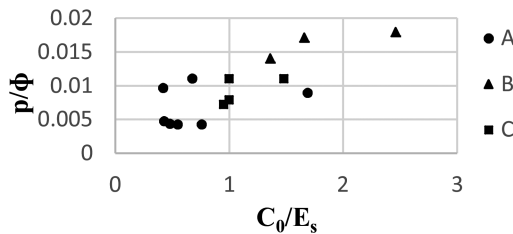Figures 7-8 show the trends found in cases A, B, C relating to (1) and (2).

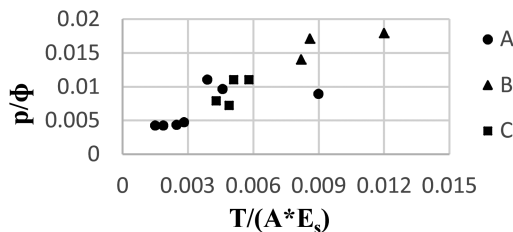Figure 7.   Left: Relationship between p/ϕ, and C_0/E_s for the cases A, B, and C of Table 1.

Figure 8.   Right: Relationship between p/ϕ and $T/(A*E_s)$ for the cases A, B, and C of Table 1.

The main problem, with TBM operation, is, however, the average monthly progression, by far lower than the net progression rate, being affected by idle time due to: machine launching time, stability problems, important machine repairs, ordinary maintenance, tools replacement and regripping time. The ratio between the production time and the total time is the U.C. In the cases examined, the U.C. averages 0.38. A low U.C. value implies the greater difficulty of the work, and this is generally due to stability problems. In the case of inclines, the U.C. it is generally smaller than horizontal tunnels due to the more difficult operating conditions.

U.C. is generally little affected by tool replacement (a certain percentage of the total time), but the number of tools replaced weighs on the operational costs.

3.2 *Tools consumption and rock abrasivity*

Tools performance is as a rule characterized by the S.T.C., the number of tools replaced per m^3 excavated. Rocks are usually characterized by abrasiveness indicators, such as the NCB Indenter index (Szlavin 1971), the Schimanek coefficient (Schimanek 1970), the quartz content, the indexes from drillability tests with small diameter bits, CERCHAR indices, micro-hardness and so on (Alber 2008, Deketh 2020). A clear trend may be noted in Figure 9 between S.T.C. and the rock micro-hardness (HK_{75}). The trend of the S.T.C. vs. s/q, where s is the flattened surface (mm^2) of the bit after one minute of drilling and q is the volume (mm^3) of the rock drilled during the same time, appears less significant in Figure 10: the rocks tested fall into two broad families: scarcely abrasive at left (sedimentary rocks), and abrasive at right (volcanic or highly metamorphosed rocks). The dispersion still observed inside each group is due to machine and tools variability and to reasons tentatively explained in the following.
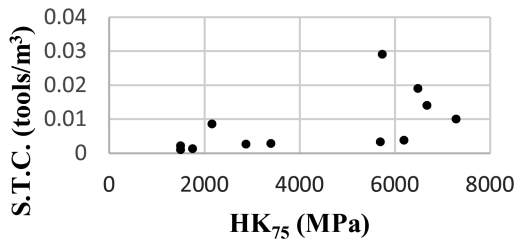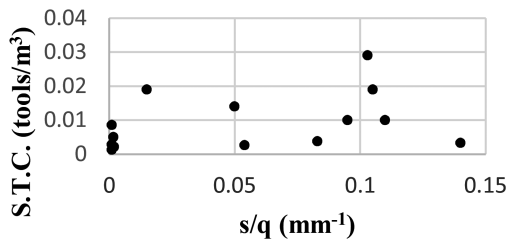

Figure 9. S.T.C. vs HK_{75}.

Figure 10. S.T.C. vs s/q.

3.3 *Relative rock hardness characterization*

As previously pointed out, the consumption of tools depends on various factors besides the abrasiveness of the rock, among which are important C_0 (West 1989) and the thrust, the latter probably due to the C_0/thrust interrelation. Some additional considerations can be made to summarize: the metal hardness, though is not so widely scattered as rock hardness, is considerably different from one case to another, and, for the same metal, from a point to another of the same specimen (the hardness discrepancy from the softest to the hardest point of the same tool can be more than 100%); quite often the tools are not purchased from manufacturers, but rather from local suppliers, which can change even during the excavation of the same tunnel; this gives rise to some uncertainty on the metal type; the diagrams refer to the metal layer, some mm thick (up to 1 cm) that is allowed to be worn before replacement. Some tools have shown uniform hardness features in the whole cross-section, some have been found to be differentially hardened, with a softer (but more resilient) core and a harder surface layer; these features apparently are important in determining the resistance to breakages rather than to pure wear (Hood & Alehossein 2000).

Of course, the specific tool consumption also depends on the machine parameters. The example in Figure 11 shows, for the cases examined, the influence of the average thrust on this parameter: as the thrust increases the specific consumption of tools increases. However, this simple statement hides a more complex phenomenon that requires to be better discussed since different factors play an important role on the wear. Firstly, the increase in thrust, considering a given penetration (corresponding to a given forward speed), is commonly performed when encountering a harder rock. In any case, the thrust cannot be indefinitely increased (due to mechanical constraints of the cutters and/or machine advancement system), consequently the penetration decreases above a certain rock strength, therefore more machine-head revolutions are necessary to cover the feed unit. Secondly, the hardness of cutting rings should also be considered for the wear phenomenon, since it is possible that by increasing the thrust, the embrittlement phenomenon also increases with a consequent increase in wear. Finally, the direction of advance of the machine and the presence of water during the excavation process also play an important role in wear. In conclusion, with reference to Figure 11, it can be hypothesized that the increase in S.T.C. could be due to the increase in the machine-head revolutions, as well as the increase in the embrittlement phenomenon. As for the last two factors, no information is available on the presence of water, while only a comparison between projects with differently oriented heading directions could highlight the important role of this factor on the tools wear. Concluding, to limit the wear, it is necessary to accept more limited performance in terms of advancement of the TBM.
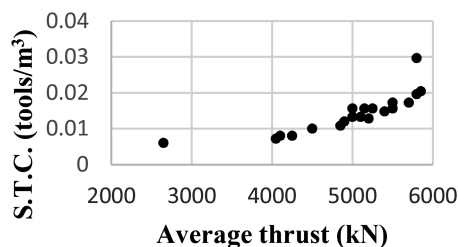

Figure 11.   S.T.C. vs average thrust.

4   CONCLUSION

Quantitative characterization of rock/metal pairs mechanically interacting at a small size scale was developed and is under test in several metals wear problems: tools' lifetime depends in fact on a great number of factors, from the rock to the tool, to the machine and to the way the machine itself is operated (Oggeri & Oreste 2012). Therefore, referring only to "rock abrasivity" is an oversimplification since the rock strength, the embrittlement phenomenon, the presence of water and the direction of advancement as a function of the orientation of the discontinuities should also be considered. All factors, however, in principle, can be either known from the results of measurements, or at least reasonably guessed in advance. The criterion here investigated relies on the knowledge of three indicators, two of them at the micro-scale (rock micro-hardness, metal micro-hardness), and one at the centimetric-decimetric scale (rock compression strength), all of them correlated to tools' life and allowing to express semi-quantitative forecasts. It is not expected that such a characterization alone can reliably predict the useful life of the metal parts of the machines, but rather that part of the metal damage can properly be ascribed to fine wear; in any case, the indicator provided by the frequency distribution R can be combined with more classical strength indicators to provide a complete picture of the effects of the metal/rock interaction on the metal.

REFERENCES

Alber, M. 2008. Stress dependency of the Cerchar abrasivity index (CAI) and its effects on wear of selected rock cutting tools. *Tunnelling and Underground Space Technology* 23(4): 351–359.

Bai, H., Zhong, L., Kang, L., Liu, J., & Xu, Y. 2021. A review on wear-resistant coating with high hardness and high toughness on the surface of titanium alloy. *Journal of Alloys and Compounds* 882: 160645.

Cardu, M., & Giraudi, A. 2012. Metal-rock pair characterization in excavation engineering. *Journal of the Southern African Institute of Mining and Metallurgy* 112(5): 379–386.

Deketh, H.J.R. 1995. *Wear of rock cutting tools: laboratory experiments on the abrasivity of rock*. London: CRC Press.

Di Giovanni, A., Todaro, C., Cardu, M., Bianchini, S., & Forfori, B. 2022. Laboratory Test Campaign Aimed at the Analysis of an Uncommon Wear Phenomenon in a Marble Quarry. *Applied Science* 12: 2264. https://doi.org/10.3390/app12042264

Frisa Morandini, A. & Mancini, R. 1982. Application of microhardness tests to the technical evaluation of dimension stones. *Proc. 4th Int. Congr. IAEG, New Delhi*, *1982*, 6: 321–331.

Hood, M., & Alehossein, H. 2000. A development in rock cutting technology. *International journal of rock mechanics and mining sciences* 37(1-2): 297–305.

Mancini, R., Cardu, M., Fornaro, M., Linares, M. 1993. Scale effects in the "micro-scale" rock mechanics problems. *II Int. Workshop on Scale effects in Rock Mines, Lisbon*, 151–158.

Oggeri, C., & Oreste, P. 2012. The wear of tunnel boring machine excavation tools in rock. *American Journal of Applied Sciences* 9(10): 1606.

Oñate Salazar, C.G., Martinelli, D., Todaro, C., Luciani, A., Boscaro, A., Peila, D. 2016a. Preliminary study of wear induced by granular soil on metallic parts of EPB tunnelling machines. *GEAM* 148: 67–70.

Oñate Salazar, C.G., Martinelli, D., Todaro, C., Peila, D., & Boscaro, A. 2016b. Study of wear in conditioned granular soil by using a new test device. *In Proceedings of the World Tunnel Congress 2016, San Francisco, CA, USA, 22–28 April 2016*, 3: 2445–2454.

Oñate Salazar, C.G., Todaro, C., Bosio, F., Bassini, E., Ugues, D., & Peila, D. 2018. A new test device for the study of metal wear in conditioned granular soil used in EPB shield tunnelling. *Tunnelling and Underground Space Technology* 73: 212–221. https://doi.org/10.1016/j.tust.2017.12.014.

Pal Dey, S.C.D.S. & Deevi, S.C. 2003. Single layer and multilayer wear resistant coatings of (Ti, Al) N: a review. *Materials Science and Engineering A 342*(1-2): 58–79.

Ribacchi, R., & Fazio, A.L. 2005. Influence of rock mass parameters on the performance of a TBM in a gneissic formation (Varzo Tunnel). *Rock mechanics and rock engineering* 38(2): 105–127.

Schimanek J. & Knatz H. 1970. Der Einfluss des Gesteinaufbaus auf die Schnittgesteinwindikeit und den Meisselversleiss. *Glueckauf* 106: 274–278.

Szlavin, J. 1971. Relationships between some physical properties of stone determined by Laboratory tests. *International Journal of Rock Mechanics and Mining Science* 11(2): 57–66.

Todaro, C., Di Giovanni, A., Oñate Salazar, C.G., Martinelli, D. 2022. The soil abrasion test apparatus: a literature review. *GEAM*, in press.

West, G. 1989. Rock Abrasivity testing for tunnelling. *Intl J of Rock Mech & Mining Sci & Geomechanic Abs*. 26(2): 151–160.